

High-precision optical heterodyne interferometric dilatometer for determining absolute CTE of EUVL materials

Yoshimasa Takeichi^{*a}, Iwao Nishiyama^a, Naofumi Yamada^b

^aEUV Process Technology Research Laboratory,
Association of Super-Advanced Electronics Technologies (ASET)
c/o NTT Atsugi R&D Center, 3-1 Morinosato Wakamiya, Atsugi, Japan 243-0198

^bNational Institute of Advanced Industrial Science and Technology (AIST)
National Metrology Institute of Japan (NMIJ)
AIST Central-3, 1-1-1 Umezono, Tsukuba-shi, Ibaraki, Japan, 305-8563

ABSTRACT

The low-thermal-expansion materials (LTEMs) used in extreme ultraviolet lithography (EUVL) must have an ultralow coefficient of thermal expansion (CTE) on the order of 10^{-9} K^{-1} . Unfortunately, the resolution of commercial dilatometers is too low to accurately measure the properties of LTEMs for EUVL. So, we have developed a practical dilatometer tailored to meet EUVL requirements. It is based on the double-path heterodyne interferometer technology developed by AIST¹. This technology has the advantage of providing absolute CTE measurements, which means direct measurement of the change in specimen length with an interferometer. The design of the dilatometer has been optimized to yield high-precision measurements, and it should enable displacement measurements to be made with a resolution of better than one nanometer.

Keywords: LTEM, EUVL, CTE, optical heterodyne interferometer, optics, mask substrate

1. INTRODUCTION

1.1. Need of metrology for EUVL LTEMs

Even small variations in the thermal expansion of the optics and mask substrate during EUVL cause errors in a printed pattern. In order to eliminate this problem, EUVL requires a material with a much lower CTE than quartz, which is commonly used in conventional optical lithography. More specifically, the SEMI standards specify a CTE of less than ± 5 ppb/K for a temperature change between 19°C and 25°C. One LTEM candidate is low-thermal-expansion glass. Amorphous glass and glass ceramics are typical LTEMs; and ULE®²⁻³ and ZERODUR®⁴⁻⁵ are well-known commercial LTEMs. The increasing interest in EUVL has led many material suppliers to launch LTEM development projects. A greater number of participating companies should lead to higher-quality materials, lower costs, and faster progress in R&D. However, the fact that there are no commercial dilatometers with a measurement resolution on the order of 1 ppb/K is an obstacle to research in this field. So, there is a strong demand among LTEM suppliers for a metrology that suits EUVL requirements.

1.2. Metrology development scheme

In 2003, a metrology development team was formed. It consists of the Association of Super-Advanced Electronics Technologies (ASET), the National Institute of Advanced Industrial Science and Technology (AIST), and companies interested in EUVL LTEMs: Asahi Glass Co. Ltd., Ohara Inc., Kyosera Co. Ltd., Shin-Etsu Chemical Co. Ltd., Toshiba Ceramics Co. Ltd., Tosho Co. Ltd., and Nihon Seratec Co. Ltd. The goal was the development of a practical dilatometer with a resolution of 1 ppb/K (repeatability: 3σ). AIST possesses high-precision CTE metrology based on an optical heterodyne interferometer. It has the advantage of providing absolute CTE measurements, which means the direct measurement of the change in sample length with an interferometer. We constructed a dilatometer using this technology as a foundation.

takeichi@aset-euv.jp; +81-46-270-6688, Fax: +81-46-270-6699

2. METHODOLOGY

2.1. Principle of measurement

AIST investigated ways to improve the accuracy of material characterization and developed a new CTE metrology. In this metrology, the CTE is obtained by measuring how much the length of a sample changes for a precisely controlled change in temperature. The CTE, α , in units of inverse Kelvins is given by

$$\alpha = \frac{\Delta L}{L_0} \cdot \frac{1}{\Delta T} \quad , \quad (1)$$

where L_0 is the initial sample length, ΔT is the change in temperature, and ΔL is the change in sample length.

Since our focus is on CTE metrology for LTEMs, we need to measure very small changes in length. Optical interferometry⁶⁻⁷ is commonly used for this purpose. Fig. 1 shows a schematic diagram of the double-path optical heterodyne interferometer developed by AIST. The system is based on two key technologies. One is an optical heterodyne interferometer, which is the type of interferometer that provides the highest resolution⁸⁻¹¹ because it detects a change in sample length as a phase difference in light, which is then converted to an electrical output signal. The other is a double-path interferometer, which increases the sensitivity to changes in length by a factor of four and cancels out the tilt of a sample.

The principle of measuring a change in length with an optical heterodyne interferometer is as follows: E_r and E_s are the electric-field components of two laser beams with different frequencies. They are given by

$$E_r = a_r \cos(2\pi f_r t + \phi_r) \quad (2)$$

$$E_s = a_s \cos(2\pi f_s t + \phi_s) \quad , \quad (3)$$

where a_r and a_s are the amplitudes, f_r and f_s are the frequencies, and ϕ_r and ϕ_s are the phases of the two beams. The intensity, I , of the superimposed beams is then

$$I = \langle |E_s + E_r|^2 \rangle \quad (4)$$

$$= \frac{a_s^2 + a_r^2}{2} + 2a_s a_r \cos\{2\pi(f_s - f_r)t + (\phi_s - \phi_r)\} \quad (5)$$

$$= \frac{a_s^2 + a_r^2}{2} + 2a_s a_r \cos\{2\pi f_b t + \Delta\phi\} \quad , \quad (6)$$

where f_b and $\Delta\phi$ are the beat frequency and phase difference between E_r and E_s , respectively. An optical heterodyne interferometer uses two pairs of laser beams with different frequencies. One pair constitutes the reference light, and the other is used for measurement. For the reference light, the phase difference is constant throughout a measurement because the optical path length remains the same. For the measurement light, the phase difference changes as the optical path length changes due to the thermal expansion or contraction of a sample. The change in sample length is obtained from the formula

$$\Delta(\phi_s - \phi_r) = \frac{2\pi\Delta L}{\lambda} \quad , \quad (7)$$

where the left side is the change in the phase difference between the reference and measurement light. In addition, the resolution of phase-difference detection is less than 1/1000 of a fringe, which is equivalent to a resolution of less than one nanometer for length measurements.

3. DESIGN AND MANUFACTURE OF THE DILATOMETER

3.1. Design of dilatometer

In order to optimize the design of the dilatometer for high precision, the uncertainty factors involved were investigated and the key hardware technologies were considered. The factors determining the overall uncertainty of a CTE measurement⁹ are contained in the following formula:

$$\delta\alpha_{total} = \left(\frac{\partial}{l}\right)_{sp} \alpha + \left[\delta\left(\frac{\partial}{l}\right)\right]_{\Delta L} \frac{1}{\Delta T} + \left[\frac{\delta(\Delta T)}{\Delta T}\right] \alpha, \quad (8)$$

where the first term is related to sample length (L); the second, to the change in sample length (ΔL); and the third, to the change in temperature (ΔT). It is possible to measure the length of a sample with an accuracy of tens of micrometers, and the contribution of this factor to the uncertainty is on the order of a few parts per trillion. So, the influence of the first term on the overall uncertainty is quite small.

The second term of (8) can be expanded into

$$\left[\delta\left(\frac{\partial}{l}\right)\right]_{\Delta L} = \left[\delta\left(\frac{\partial}{l}\right)\right]_{las} + \left[\delta\left(\frac{\partial}{l}\right)\right]_{fri} + \left[\delta\left(\frac{\partial}{l}\right)\right]_{tilt} + \left[\delta\left(\frac{\partial}{l}\right)\right]_{mir} + \left[\delta\left(\frac{\partial}{l}\right)\right]_{air}, \quad (9)$$

where the terms on the right side, in order, are related to the stability of the laser wavelength, measurement of the phase difference, the difference in sample length due to the tilt of the sample during measurement, the uniformity of the reflector thickness, and fluctuations in the refractive index of air. Each of these terms is discussed below.

The first term of (9) can be written

$$\left[\delta\left(\frac{\partial}{l}\right)\right]_{las} = \frac{4L_0}{\lambda} \cdot \delta\lambda, \quad (10)$$

where L_0 is the initial sample length, and $4L_0$ is the optical path difference (OPD). The contribution of this term to the uncertainty is estimated to be 0.1 ppb/K when the stability of the laser wavelength is 10^{-9} .

The second term of (9) can be written

$$\left[\delta\left(\frac{\partial}{l}\right)\right]_{fri} = \delta(\Delta(\phi_1 - \phi_2)) \cdot \frac{\lambda}{2\pi} \cdot \frac{l}{l_0}, \quad (11)$$

The accuracy of the phase-difference measurement is determined by the performance of the lock-in amplifier. The contribution of this term to the uncertainty is estimated to be 0.1 ppb/K for a lock-in amplifier with an accuracy of 0.05° .

The third term of (9) is given by

$$\left[\delta\left(\frac{\partial}{l}\right)\right]_{tilt} = L_0 \times (1 - \cos \theta) \cong L_0 \theta^2, \quad (12)$$

Figure 2 is a photograph of a sample attached to the sample stand with optical cement. Together they form an inverted T-shape. This structure was deemed best for avoiding sample tilt. However, one potential problem is that heat could deform the contact plate and Peltier device under the stand, causing the sample to tilt. For a sample tilt of 30 seconds, for instance, the contribution to the uncertainty is estimated to be 1 ppb/K, which is large.

The fourth term of (9) can be written

$$\left[\delta \left(\frac{\delta}{l} \right) \right]_{mir} = \delta t_{mir} \cdot \alpha_{mir} \quad , \quad (13)$$

where δt_{mir} and α_{mir} are the uniformities of the thickness of the reflecting film and the CTE, respectively. The thermal expansion of the reflecting film itself produces a difference in thickness between the film on the top of a sample and the film on the sample stand, thus giving rise to error in the CTE measurement. The contribution of this factor to the uncertainty is below 1 ppt for film with a thickness of 600 nm and a uniformity of 20%.

The fifth term of (9) is the contribution to the uncertainty from fluctuations in the refractive index of air. This factor can be made negligible by performing measurements in a vacuum chamber.

The uncertainty factors⁸ related to the control and determination of the temperature are

$$\left[\frac{\delta(\Delta T)}{\Delta T} \right]_T = \left[\frac{\delta(\Delta T)}{\Delta T} \right]_{res} + \left[\frac{\delta(\Delta T)}{\Delta T} \right]_{flc} + \left[\frac{\delta(\Delta T)}{\Delta T} \right]_{cal} \quad , \quad (14)$$

where the terms on the right side, in order, are for the resolution of temperature measurements, temperature fluctuations inside a sample, and the calibration error of the sensors. The sizes of the errors are 1 mK (for a Pt thermistor), 50 mK (result of preliminary experiment), 5 mK (guaranteed performance), respectively. The total error for temperature control is mainly determined by the second term of (14), and that contribution to the uncertainty is estimated to be 0.1 ppb/K

3.2. Construction of dilatometer

As described above, the uncertainty factors were investigated, and their contributions were estimated under typical conditions. The results, summarized in Table 1, reveal the key points that need to be considered in the design of a dilatometer. The light source for the interferometer is a frequency-stabilized laser (stability: 10^{-11}). The structure of the components of the dilatometer around a sample is optimized to suppress sample tilt. Figure 3 illustrates the internal structure of the sample chamber. In addition, CLEARSERAM Z-HS (OHARA Inc.) is used for the support that holds the Peltier device.

Constant-temperature blocks and a Peltier device keep the temperature inside a sample uniform. Figure 4 illustrates the precision thermal control unit for a sample. The sample temperature is mainly determined by the constant-temperature blocks; and the thermal conduction from the sample to the contact plate is regulated by the Peltier device to improve the uniformity of the sample temperature.

These component technologies have been combined in the construction of a dilatometer. The flow chart in Fig. 5 shows how the system operates. A personal computer (PC) automatically controls the temperature and takes measurements. The change in sample length is determined using a digital lock-in amplifier; and the PC automatically collects the data. The photographs in Fig. 6 show (a) the vacuum chamber, (b) the optics of the interferometer, and (c) the inside of the vacuum chamber.

4. RESULTS

4.1. Measurement of CTE of quartz

The CTE of commercial quartz was measured to test the capabilities of the dilatometer. The temperature was cycled through the temperatures 19°C, 22°C, and 25°C; and the phase difference was measured at each step. The holding time at each temperature was 10 hours. The results in Fig. 7 show (a) phase difference, (b) average sample temperature, and (c) uniformity of sample temperature. The CTE was calculated from the change in phase difference for each change in temperature, and the results are shown in Table. 2. The average CTE was found to be about 0.46 ppm for the temperature change between 19°C and 22°C, and about 0.47 ppm for the change between 22°C and 25°C. These values are consistent with the known CTE of quartz. In addition, the temperature uniformity inside a sample during a measurement was about 60 mK or less. The CTEs of LTEMs are now being measured, and the results will be presented in a future report.

5. CONCLUSIONS

A dilatometer specialized to meet the requirements of EUVL has been developed by ASET, AIST and a group of LTEM suppliers. It performs absolute measurements using a double-path optical heterodyne interferometer. The uncertainty factors involved in CTE measurements were investigated, and the results were used to optimize the design. A prototype was constructed and used to measure the CTE of quartz. The measurements were successful, and the values obtained are consistent with known values. Plans call for a rigorous evaluation of the performance of the dilatometer

ACKNOWLEDGEMENT

This work was supported by the New Energy and Industrial Technology Development Organization (NEDO).

REFERENCES

1. Okaji M., Yamada N., *Metrologia*, 2000, 37, 165-171.
2. Kenneth E.Hrdina, et al. "Characterization and Characteristics of a ULE Glass Tailored for the EUVL Needs", *Proc. SPIE Vol.4688*, 454-461, 2002.
3. Kenneth E.Hrdina, et al. "Measuring and tailoring CTE within ULE Glass", *Proc. SPIE Vol.5037*, 227-235, 2003.
4. Ina Mitra, et al. "Thermal Expansion Behavior of Proposed EUVL Substrate Materials", *Proc. SPIE Vol.4688*, 462-468, 2002.
5. Ina Mitra, et al. "Improved Materials meeting the demands for EUV Substrates", *Proc. SPIE Vol.5037*, 219-226, 2003.
6. S J Bennett, "An Absolute interferometric dilatometer", *J. Phys. E: Sci. Instrum.* 10, 525-530, 1977.
7. R B Roberts, "Absolute dilatometry using a polarization interferometer", *J. Phys. E: Sci. Instrum.* 14, 1386-1388, 1981.
8. M. Okaji et al. "High-resolution multifold path interferometers for dilatometric measurements", *J. Phys. E: Sci. Instrum.* 16, 1983.
9. M. Okaji et al. "A practical measurement system for the accurate determination of linear thermal expansion coefficients", *J. Phys. E: Sci. Instrum.* 17, 1984.
10. M. Okaji et al. "A high-temperature dilatometer using optical heterodyne interferometry", *J. Phys. E: Sci. Instrum.* 20, 1987.
11. M. Okaji et al. "Laser interferometric dilatometer at low temperatures: application to fused silica SRM739", *Cryogenics* (1995) 35, 887-891, 1995.

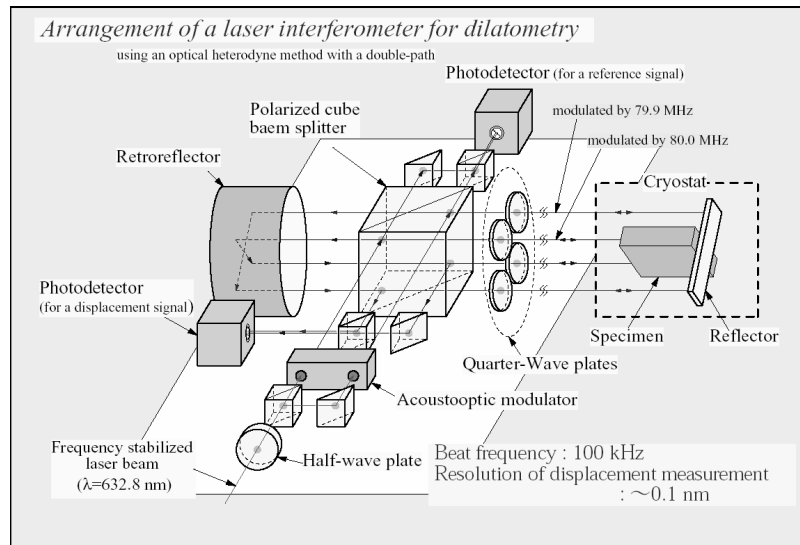


Fig. 1. Schematic diagram of high-precision CTE measurement equipment developed by AIST. It is used for calibration.

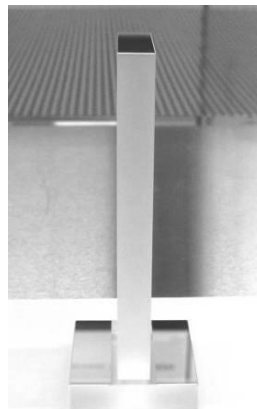


Fig. 2. Photograph of quartz sample for CTE measurement.

Table 1. Uncertainty factors and estimated values for CTE measurements.
 α : 5 ppb/K; sample length: 100 mm; ΔT : 2 K

Uncertainty factor	Typical value	Contribution to uncertainty [K-1]
i) Sample length measurement	1.0E-5 [m]	5.00E-13
ii) Sample length diversification measurement(overall)		1.54E-09
Laser wave-length stability (Random)	1.0E-9	2.00E-10
Phase difference measurement (Random)	0.05 [deg]	4.37E-10
Sample inclination (Systematic)	30 [s]	1.06E-09
Uniformity of reflector thickness (Systematic)	90 [nm]	1.08E-12
iii) Temperature control & decision	0.1 [K]	2.50E-10
Total uncertainty(i + ii + iii)		1.79E-09

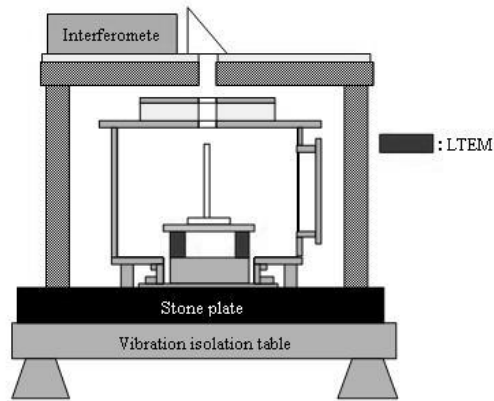


Fig. 3. Internal structure of sample chamber.

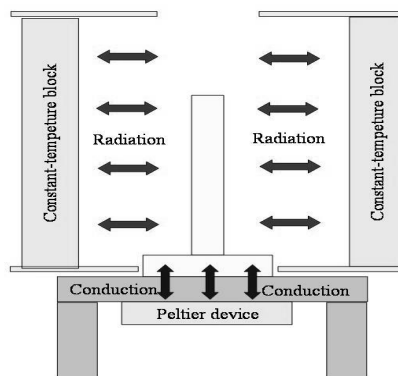


Fig. 4. Schematic diagram of precision thermal-control unit for sample.

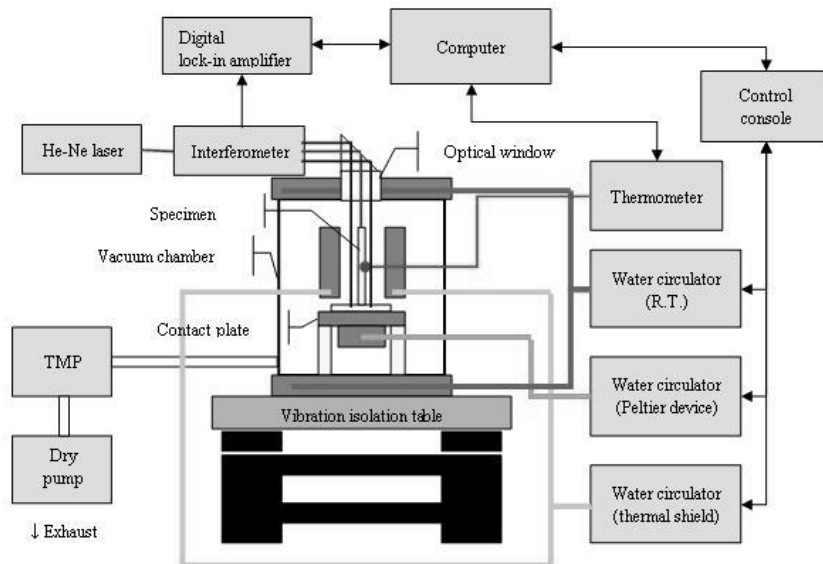


Fig. 5. Flow chart showing operation of high-precision CTE measurement system.

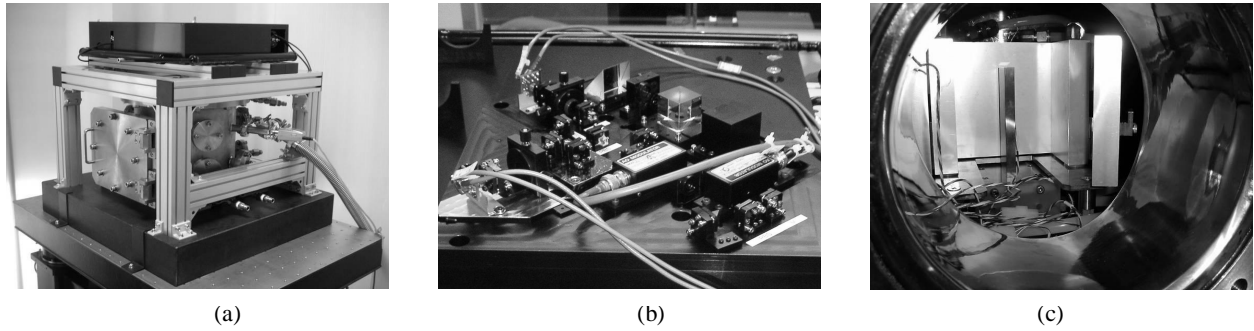


Fig. 6. Photographs of high-precision CTE measurement system: (a) sample chamber and interferometer unit, (b) optics of interferometer, and (c) interior of sample chamber.

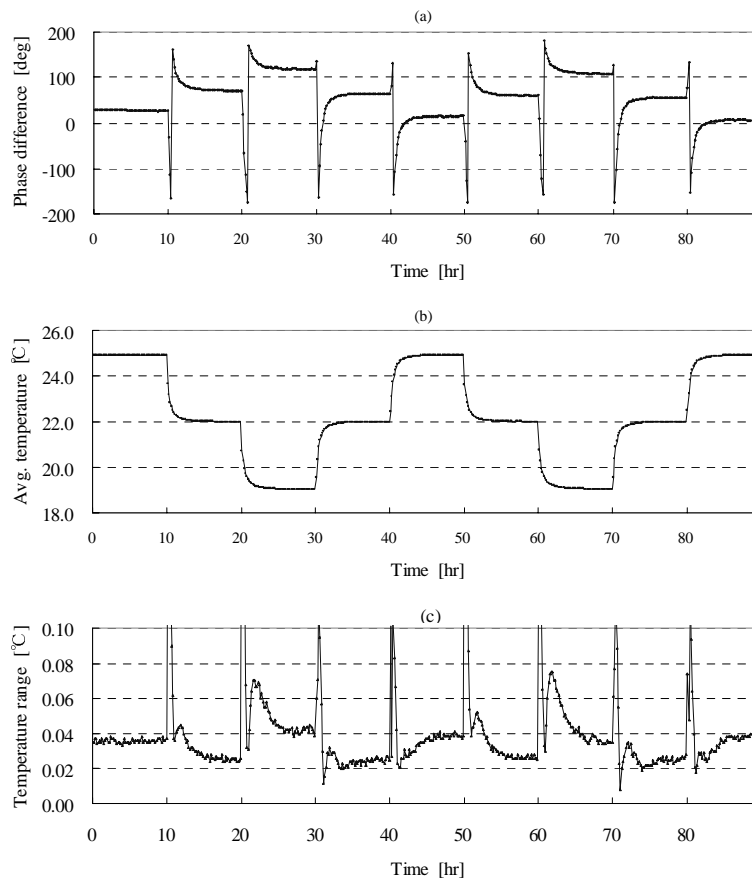


Fig. 7. CTE measurement data for quartz sample: (a) phase difference, (b) average temperature of sample, and (c) range of sample temperatures.

Table 2. Results for two measurements of CTE of quartz sample. [ppm]

T1	T2	Meas.1	Meas.2	Δ (Meas.2-Meas.1)
19	22	0.460	0.464	0.004
22	25	0.470	0.471	0.001